Modelling and Simulation of a Bottling Plant using Hybrid Petri Nets *

Alessandro Giua (†), Maria Teresa Pilloni (‡), Carla Seatzu (†)

(†) Dip. Ingegneria Elettrica ed Elettronica, Università di Cagliari,
Piazza d'Armi, 09123 Cagliari, Italy. {giua,seatzu}@diee.unica.it
(‡) Dip. Ingegneria Meccanica, Università di Cagliari,
Piazza d'Armi, 09123 Cagliari, Italy. pilloni@dimeca.unica.it

Abstract

In this paper we use First–Order Hybrid Petri nets (FOHPN), an hybrid model that combines fluid and discrete event dynamics, to model the concurrent activities of manufacturing systems. In particular we consider an existing mineral water bottling plant and we show how the FOHPN model is extremely suited to describe the high-throughput production lines, that are one of the main components in the considered plant. Some variations with respect to the previous definition of the FOHPN model are also introduced here to better describe the behavior of the conveyor lines. Finally, we show that, thanks to the fluid approximation of some discrete-event dynamics, the considered plant may also be efficiently simulated using FOHPN. This also enabled us to identify, among the most commonly used configurations of the plant, which are the optimal working conditions in terms of maximal throughput and net profit.

Keywords: manufacturing systems, bottling plant, discrete event systems, hybrid systems, hybrid Petri nets, First-Order Hybrid Petri nets.

*Submitted to the *International Journal of Production Research.* Contact author is Alessandro Giua.

1 Introduction

In this paper we show how *hybrid Petri nets* [13], a *hybrid model* [9] that combines fluid and discrete event dynamics, are extremely suited to model the dynamic concurrent activities of manufacturing systems and in particular, high-throughput production lines.

1.1 The considered application

In the present work, a production line of an existing plant is considered. The plant under study is the Sarda Acque Minerali (SAM) unit, a mineral water bottling plant located in southern Sardinia, at about 20 km from the city of Cagliari. The company production achieves about 110 millions of bottles per year; several formats (0.25 ℓ, 0.5 ℓ, 1 ℓ, 1.5 ℓ, 2 ℓ) of bottles are produced, filled and finally sold, both with still mineral and sparkling water. Moreover four different mineral water brands are produced. One of the main characteristics of the company consists in its deep integration with Biorientati Plastici (BP), a company that produces the PET bottles which are filled by the SAM filling machines. Most of the problems presently preventing a good production management arises from the lower productivity of the BP machines with respect to the SAM machines. As a consequence, in order to ensure to the SAM filling machines the essential working continuity, BP machines must be run on longer shifts and intermediate stockpiles of the produced bottles in proper buffers had to be realized.

The target of the present work is that of presenting a *formal model* that is extremely suited to capture the main features of high-throughput production lines and the concurrent activities of the considered manufacturing system. One important feature of the proposed model consists in allowing the fluid approximation of some discrete-event dynamics. Thanks to this we have been able to efficiently simulate the behavior of a significant part of the production plant. In particular, a comparison among some working configurations often used by the plant operators, enabled us to identify which is the best configuration in terms of throughput and net profit.

The particular model considered in this paper is called *First–Order Hybrid Petri nets* (FOHPN). The Petri net model of the plant have been developed by the same authors and firstly presented in [15, 5]. Note that Hybrid and Batch Petri net models have also been used for modeling, packing and bottling plants by I. Demongodin in [12].

1.2 The considered model

Discrete Petri nets [16] are a discrete event model whose state space belongs to the set of non-negative integers. This is a major advantage with respect to other formalisms such as automata, where the state space is a symbolic unstructured set, and has been exploited to develop many analysis techniques that do not require to enumerate the state space (structural analysis) [11]. Timed discrete Petri nets, i.e., Petri nets with a timing structure associated to the transition firing, are a well studied performance model and have strong inter-relations with other models of positive systems: as an example, deterministic timed marked graphs (a subclass of Petri nets) can be studied as max-plus linear models [6, 10]; stochastic Petri nets [1] can model generalized semi-markovian processes, etc.

Recently, much work has been devoted to the extension of the classical discrete Petri net formalism to continuous Petri nets, i.e., nets obtained from discrete nets by "fluidification" [3, 19]. The advantage of "fluidification" originates from the following considerations. In many applications dealing with complex systems, e.g., high–throughput manufacturing systems an example of which is discussed in this paper, a plant has a discrete event dynamics whose number of reachable states is typically very large. The simulation and analysis of these systems require large amount of computational efforts, and problems of realistic scale quickly become analytically and computationally untractable. To cope with this problem it is possible to give a continuous approximation of the discrete event dynamics [17, 18, 20]. This has several advantages.

- Firstly, there is the possibility of considerable increase in computational efficiency, because the simulation of fluid models can often be done much more efficiently.
- Secondly, fluid approximations provide an aggregated formulation to deal with complex systems, thus reducing the dimension of the state space.
- Thirdly, the design parameters in fluid models are continuous hence there is the possibility of using gradient information to speed up optimization and perform sensitivity analysis.

Note that the discrete event dynamics that can be represented by a fluid model are usually related to the flow of materials, thus making fluid models essentially a type of *compartmental models* [9], a sub-class of *positive systems*.

It should be noted that in general different fluid approximations are necessary to describe the same system, depending on its discrete state. Thus, the resulting model can be better described as an *hybrid model*, where different dynamics are associated to each discrete state. This has lead recently to the definition of a new family of Petri net models that combine discrete and continuous subsystems into a so called hybrid Petri net [2, 13]. Note that the area of hybrid systems has received a lot of attention in the automatic control community, lately: we believe that in the next years much attention will also be devoted to hybrid positive systems, i.e., positive systems combining both discrete event and continuous dynamics, and hybrid Petri nets are a good example of this class of systems.

The hybrid Petri net model considered in this paper is called *First–Order* Hybrid Petri nets (FOHPN) because its continuous dynamics are piece-wise constant. FOHPN were originally presented in [7]. FOHPN have also been used in many application domains such as manufacturing [8] and inventory management control [14].

The rest of the paper first presents the necessary background on FOHPN and then shows in detail an example of modelling and simulation applied to a real system.

2 First–Order Hybrid Petri Nets

In this paper we use the Petri net formalism firstly presented in [7].

Net structure: A FOHPN is a structure $N = (P, T, Pre, Post, \mathcal{D}, \mathcal{C})$.

The set of *places* $P = P_d \cup P_c$ is partitioned into a set of *discrete* places P_d (represented as circles) and a set of *continuous* places P_c (represented as double circles). The cardinality of P, P_d and P_c is denoted n, n_d and n_c.

The set of *transitions* $T = T_d \cup T_c$ is partitioned into a set of discrete transitions T_d and a set of continuous transitions T_c (represented as double boxes). The set $T_d = T_I \cup T_D \cup T_S$ is further partitioned into a set of *immediate* transitions T_I (represented as bars), a set of *deterministic timed* transitions T_D (represented as black boxes), and a set of *stochastic timed* transitions T_S (represented as white boxes). The cardinality of T, T_d and T_c is denoted q, q_d and q_c.

The *pre-* and *post-incidence functions* that specify the arcs are (here $\mathbb{R}_0^+ = \mathbb{R}^+ \cup \{0\}$): $Pre, Post : P_c \times T \to \mathbb{R}_0^+$, $P_d \times T \to \mathbb{N}$. We require (*well-formed nets*) that for all $t \in T_c$ and for all $p \in P_d$, $Pre(p,t) = Post(p,t)$. This ensures that the firing of continuous transitions does not change the marking of discrete places.

The function $\mathcal{D} : T_D \to \mathbb{R}^+$ specifies the timing associated to a deterministic transition $t_j \in T_D$, i.e., its (constant) firing delay $\delta_j = \mathcal{D}(t_j)$. In the case of timed stochastic transitions, $\mathcal{D} : T_S \to \mathcal{F}$ assigns to each $t_j \in T_S$ a probability density function (pdf) that characterizes its firing delay[1].

The function $\mathcal{C} : T_c \to \mathbb{R}_0^+ \times \mathbb{R}_\infty^+$ specifies the firing speeds associated to continuous transitions (here $\mathbb{R}_\infty^+ = \mathbb{R}^+ \cup \{\infty\}$). For any continuous transition $t_j \in T_c$ we let $\mathcal{C}(t_j) = (V_j', V_j)$, with $V_j' \leq V_j$. Here V_j' represents the *minimum firing speed* (mfs) and V_j represents the *maximum firing speed* (MFS). In the following, unless explicitly specified, the mfs of a continuous transition will be $V_j' = 0$.

The *incidence matrix* of the net is defined as $C(p,t) = Post(p,t) - Pre(p,t)$. The restriction of $\boldsymbol{C}$ to P_X and T_Y ($X, Y \in \{c, d\}$) is denoted $\boldsymbol{C}_{XY}$.

A *marking* is a function that assigns to each discrete place a non-negative number of tokens, represented by black dots and assigns to each continuous place a fluid volume. A continuous place can be seen as a tank that can fill up with fluid (marking). However, we also consider some connecting elements (such as a pipe) with a zero capacity where fluid

[1]Here $\mathcal{F}$ is the set of probability density functions for a random variable that can only take non negative values, as is the case with a firing delay.

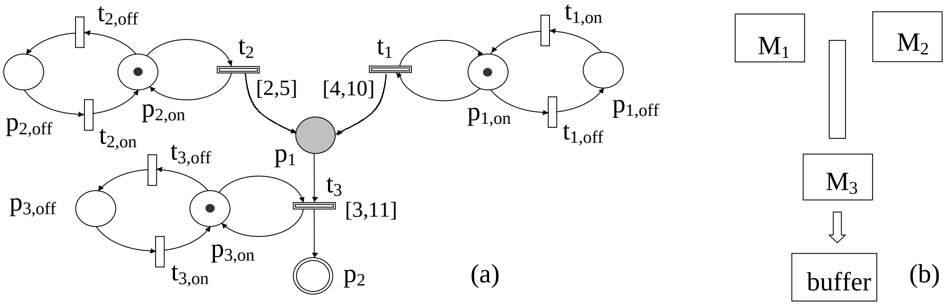

Figure 1: *A First–Order Hybrid Petri Net.*

can flow but not accumulate. Thus we partition the set of continuous places $P_c = P_0 \cup P_+$ into a set of places P_0 (represented as full dark circles) whose marking is always equal to zero (connecting elements), and a set of places P_+ (represented as double circles) whose marking may assume any nonnegative real number (tanks). Therefore $\boldsymbol{m} : \ P_+ \to \mathbb{R}_0^+$, $P_0 \to 0$, $P_d \to \mathbb{N}$. The marking of place p_i is denoted m_i, while the value of the marking at time τ is denoted $\boldsymbol{m}(\tau)$. The restriction of $\boldsymbol{m}$ to P_d and P_c are denoted with $\boldsymbol{m}^d$ and $\boldsymbol{m}^c$, respectively. An *FOHPN system* $\langle N, \boldsymbol{m}(\tau_0)\rangle$ is an FOHPN N with an initial marking $\boldsymbol{m}(\tau_0)$.

Note that in the original formalism used in [7, 8] no partition was introduced in the set of continuous places, thus $P_c \equiv P_+$, and places with a constant zero marking were modeled through zero–capacity buffers.

Example 1 Consider the net in Figure 1.a. Places $p_{1,on}$, $p_{1,off}$, $p_{2,on}$, $p_{2,off}$, $p_{3,on}$ and $p_{3,off}$ are discrete places. Places p_1 and p_2 are continuous places, with $p_1 \in P_0$ and $p_2 \in P_+$. Discrete transitions $t_{1,on}$, $t_{1,off}$, $t_{2,on}$, $t_{2,off}$, $t_{3,on}$ and $t_{3,off}$ are exponentially distributed timed transitions whose average firing rates are $\lambda_{1,on}$, $\lambda_{1,off}$, $\lambda_{2,on}$, $\lambda_{2,off}$, $\lambda_{3,on}$ and $\lambda_{3,off}$ respectively. Transitions t_1, t_2 and t_3 are continuous transitions whose mfs and MFS are specified between brackets.

The net in Figure 1.a represents the manufacturing process sketched in Figure 1.b. The three continuous transitions t_1, t_2 and t_3 represent three unreliable machines M_1, M_2 and M_3; parts produced by the first two machines are collected into a conveyor whose capacity may be assumed equal to zero, and are then sent to the third machine M_3 who processed them again before sending them to the buffer (modeled by place p_2).

In the net system in Figure 1.a the discrete part of the net represents the failure model of the machines. When place $p_{1,on}$ is marked, transition t_1 is enabled, i.e., machine M_1 is operational; when place $p_{1,off}$ is marked, transition t_1 is not enabled, i.e., the machine is down. A similar interpretation applies to the other machines. The marking represented in the net shows that initially all machines are operational and the buffer is empty. ■

Net dynamics: The enabling of a discrete transition depends on the marking of all its input places, both discrete and continuous. More precisely, a discrete transition t is *enabled* at $\boldsymbol{m}$ if for all $p_i \in {}^\bullet t$, $m_i \geq Pre(p_i, t)$, where ${}^\bullet t$ denotes the preset of transition t.

A timed transition t_j fires after being enabled for a time interval ν_j of appropriate length. In particular, if $t_j \in T_I$, $\nu_j = 0$ and t_j fires as soon as it is enabled. If $t_j \in T_D$ then $\nu_j = \delta_j$, thus t_j fires after being enabled for a time interval whose length is equal to its firing delay δ_j. Finally, if $t_j \in T_S$ then ν_j is the current sample of the associated random variable.

If a discrete transition t_j fires at a certain time instant τ^-, then its firing at $\boldsymbol{m}(\tau^-)$ yields a new marking $\boldsymbol{m}(\tau)$. For each place p_i it holds $m_i(\tau) = m_i(\tau^-) + Post(p_i, t_j) - Pre(p_i, t_j) = m_i(\tau^-) + C(p_i, t_j)$, thus we can write $\boldsymbol{m}^c(\tau) = \boldsymbol{m}^c(\tau^-) + \boldsymbol{C}_{cd}\boldsymbol{\sigma}$, $\boldsymbol{m}^d(\tau) = \boldsymbol{m}^d(\tau^-) + \boldsymbol{C}_{dd}\boldsymbol{\sigma}$, where $\boldsymbol{\sigma}$ is the *firing count vector* associated to the firing of transition t_j, i.e., $\boldsymbol{\sigma} \in \mathbb{N}^{q_d}$ and $\sigma_i = 1$ if $i = j$ else $\sigma_i = 0$.

To every continuous transition t_j is associated an instantaneous firing speed (IFS) $v_j(\tau)$. It represents the quantity of markings by time unit that fires the continuous transition at the generic time instant τ. For all τ it should be $V'_j \leq v_j(\tau) \leq V_j$, thus the IFS of each continuous transition is piecewise constant between events.

An empty continuous place p_i can be fed, i.e., supplied, by an input transition, which is enabled. Thus, as a flow can pass through an unmarked continuous place, this place can deliver a flow to its output transitions. Consequently, a continuous transition t_j is enabled at time τ if and only if all its input discrete places $p_k \in P_d$ have a marking $m_k(\tau)$ at least equal to $Pre(p_k, t_j)$, and all its input continuous places $p_i \in P_c$ satisfy the following condition: either $m_i(\tau) > 0$ or p_i is fed. If all input continuous places of t_j have a not null marking, then t_j is called *strongly enabled*, else t_j is called *weakly enabled.* Finally, transition t_j is not enabled if one of its empty input places is not fed.

We can write the equation which governs the evolution in time of the marking of a place $p_i \in P_c$ as

$$\dot{m}_i(\tau) = \sum_{t_j \in T_c} C(p_i, t_j) v_j(\tau) \tag{1}$$

where $\boldsymbol{v}(\tau) = [v_1(\tau), \ldots, v_{n_c}(\tau)]^T$ is the IFS vector at time τ. Indeed Equation (1) holds assuming that at time τ no discrete transition is fired and that all speeds $v_j(\tau)$ are continuous in τ.

The enabling state of a continuous transition t_j defines its admissible IFS v_j.

- If t_j is not enabled then $v_j = 0$.
- If t_j is strongly enabled, then it may fire with any firing speed $v_j \in [V'_j, V_j]$.
- If t_j is weakly enabled, then it may fire with any firing speed $v_j \in [V'_j, \overline{V}_j]$, where $\overline{V}_j \leq V_j$ since t_j cannot remove more fluid from any empty input continuous place $\overline{p}$ than the quantity entered in $\overline{p}$ by other transitions.

The computation of the IFS of enabled transitions is not a trivial task. We will set up in the next subsection a linear–algebraic formalism to do this. Here we simply discuss the net evolution assuming that the IFS are given.

We say that a *macro–event* occurs when: (a) a discrete transition fires, thus changing the discrete marking and enabling/disabling a continuous transition; (b) a continuous place becomes empty, thus changing the enabling state of a continuous transition from strong to weak.

Let τ_k and τ_{k+1} be the occurrence times of two consecutive macro–events as defined above; we assume that within the interval of time $[\tau_k, \tau_{k+1})$, denoted as a *macro–period*, the IFS vector is constant and we denote it $\boldsymbol{v}(\tau_k)$. Then the continuous behavior of an FOHPN for $\tau \in [\tau_k, \tau_{k+1})$ is described by $\boldsymbol{m}^c(\tau) = \boldsymbol{m}^c(\tau_k) + \boldsymbol{C}_{cc}\boldsymbol{v}(\tau_k)(\tau - \tau_k)$, $\boldsymbol{m}^d(\tau) = \boldsymbol{m}^d(\tau_k)$.

Example 2 Let us consider again the net system in Figure 1.a. Discrete transitions $t_{1,off}$, $t_{2,off}$ and $t_{3,off}$ are enabled, while transitions $t_{1,on}$, $t_{2,on}$ and $t_{3,on}$ are disabled. Continuous transitions t_1 and t_2 are strongly enabled, while transition t_3 is weakly enabled because it has an empty input continuous place p_1 that is fed by transitions t_1 and t_2. ■

We use linear inequalities to characterize the set of *all* admissible firing speed vectors $\mathcal{S}$. Each IFS vector $\boldsymbol{v} \in \mathcal{S}$ represents a particular mode of operation of the system described by the net, and among all possible modes of operation, the system operator may choose the best according to a given objective.

They form a convex set described by linear equations.

Definition 1 (admissible IFS vectors) *Let $\langle N, \boldsymbol{m} \rangle$ be an FOHPN system with n_c continuous transitions and incidence matrix $\boldsymbol{C}$. Let $T_{\mathcal{E}}(\boldsymbol{m}) \subset T_c$ ($T_{\mathcal{N}}(\boldsymbol{m}) \subset T_c$) be the subset of continuous transitions enabled (not enabled) at $\boldsymbol{m}$, and $P_{\mathcal{E}}(\boldsymbol{m}) = \{p \in P_+ \mid m_p = 0\}$ be the subset of empty continuous places in P_+. Any* admissible IFS vector $\boldsymbol{v} = [v_1, \cdots, v_{n_c}]^T$ *at $\boldsymbol{m}$ is a feasible solution of the following linear set:*

$$\begin{cases} (a) & V_j - v_j \geq 0 & \forall t_j \in T_{\mathcal{E}}(\boldsymbol{m}) \\ (b) & v_j - V'_j \geq 0 & \forall t_j \in T_{\mathcal{E}}(\boldsymbol{m}) \\ (c) & v_j = 0 & \forall t_j \in T_{\mathcal{N}}(\boldsymbol{m}) \\ (d) & \sum_{t_j \in T_{\mathcal{E}}} \boldsymbol{C}(p, t_j) \cdot v_j \geq 0 & \forall p \in P_{\mathcal{E}}(\boldsymbol{m}) \\ (e) & \sum_{t_j \in T_{\mathcal{E}}} \boldsymbol{C}(p, t_j) \cdot v_j = 0 & \forall p \in P_0 \end{cases} \tag{2}$$

Thus the total number of constraints that define this set is

$$2 \ card\{T_{\mathcal{E}}(\boldsymbol{m})\} + card\{T_{\mathcal{N}}(\boldsymbol{m})\} + card\{P_{\mathcal{E}}(\boldsymbol{m})\} + card\{P_0\}\,.$$

The set of all feasible solutions is denoted $\mathcal{S}(N, \boldsymbol{m})$. ■

Constraints of the form (2.a), (2.b), and (2.c) follow from the firing rules of continuous transitions. Constraints of the form (2.d) follow from (1), because if a continuous place

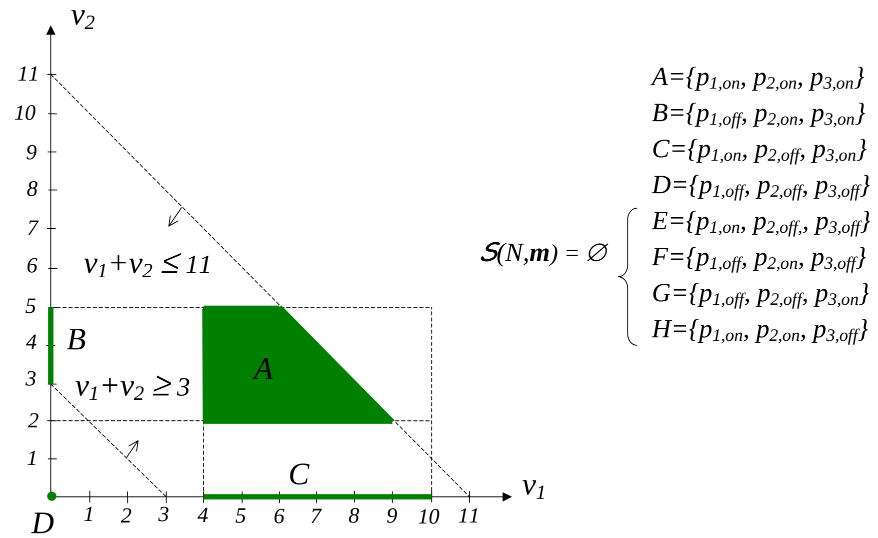

Figure 2: *The set of admissible IFS for transitions t_7 and t_8 in Figure 1.*

is empty then its fluid content cannot decrease. Constraints of the form (2.e) follow from the fact that places in P_0 should always be empty by definition. Note that if $V_i' = 0$, then the constraint of the form (2.b) associated to t_i reduces to a non–negativity constraint on v_i.

Example 3 Let us consider the net N in Figure 1.a. As already discussed above the set of admissible IFS depends on the actual marking of the net. In the particular case at hand, the set of macro–periods is uniquely characterized by the discrete marking of the net because $P_{\mathcal{E}}(\boldsymbol{m}) = \emptyset$.

In Figure 2 we have reported the set of admissible IFS for transitions t_1 and t_2. Note that, being $m_1(\tau) = 0$ for all time instants τ, it follows that $v_3(\tau) = v_1(\tau) + v_2(\tau)$ for all τ, thus the dark areas in Figure 2 completely describe the set $\mathcal{S}(N, \boldsymbol{m})$ for all $\boldsymbol{m}$.

The sets of reachable discrete markings have been characterized by explicitly enumerating the set of marked discrete places and have been denoted as A, B, $\cdots$, H. As an example, $A = \{p_{1,on}, p_{2,on}, p_{3,on}\}$ is representative of the discrete marking $m(p_{1,on}) = m(p_{2,on}) = m(p_{3,on}) = 1$ and $m(p_{1,off}) = m(p_{2,off}) = m(p_{3,off}) = 0$.

The plot in Figure 2 has been obtained considering that whenever transitions t_1 and t_2 are enabled, it should be $4 \leq v_1 \leq 10$ and $2 \leq v_2 \leq 5$, respectively. Moreover, whenever transition t_3 is enabled it should be $3 \leq v_3 \leq 11$, thus implying two additional constraints in the set of IFS of transitions t_1 and t_2, i.e., $3 \leq v_1 + v_2 \leq 11$.

The set A denotes the macro–period in which all machines are operational. The larger dark region in Figure 2 is representative of the set of admissible IFS for this discrete marking. Note that an operating mode with both transitions t_1 and t_2 firing at their MFS is not allowed (point $(10, 5)$ does not belong to this region).

The macro–period B corresponds to the situation in which t_2 and t_3 are enabled while t_1 is not enabled. We may observe that t_2 may never fire at its mfs. Similar considerations may be repeated for the macro–period C with the only difference that in this case the admissible IFS of t_3 imposes no additional constraint in the IFS of t_1 being $[V_1', V_1] = [4, 10] \subset [V_3', V_3] = [3, 11]$.

Macro–period D corresponds to the situation in which no machine is operational, i.e., no continuous transition may fire and the discrete places $p_{1,off}$, $p_{2,off}$ and $p_{3,off}$ are marked.

Finally, let us observe that no operational mode exists when the set of marked discrete places is any of the sets E, F, G and H. As an example, let us consider the set F. In this case the set of admissible IFS is

$$\mathcal{S}(N, \boldsymbol{m}) = \begin{cases} v_1 = 0 \\ 2 \leq v_2 \leq 5 \\ v_3 = 0 \\ v_1 + v_2 - v_3 = 0 \end{cases} = \begin{cases} v_1 = 0 \\ 2 \leq v_2 \leq 5 \\ v_3 = 0 \\ v_2 = 0 \end{cases} = \emptyset.$$

Similar conclusions may be drawn for the sets E, G and H. Physically this means that when a machine is operational then its IFS should be within its mfs and its MFS. If its mfs is strictly positive and we want its IFS to be null, then the machine should be switched off. ■

Once the set of all admissible IFS vectors has been defined, we need a procedure to select one among them. One possible way of computing an optimal IFS vector consists in introducing an objective function that may be representative of a global performance index and solving the corresponding optimization problem with constraint set given by (2).

3 Modeling plant subsystems with FOHPN

In this section we present the Petri net model of the most important elementary modules of a bottling plant, namely transportation lines and switches, machines and buffers, that are then put together to make the whole Petri net model of a part of a real production plant.

We first introduce a novel elementary module of Petri nets, named *macro transition*, that will be useful in the following to get a more compact representation of the other elementary modules. A macro transition is represented with a large rectangle with some continuous transitions inside to denote that only one continuous transition at a time may be enabled. In such a way we can omit the representation of the discrete part of the net. An example of macro transition is reported in Figure 3 in the case of two continuous transitions. When $p_{on,1}$ is marked, transition $t_{c,1}$ may fire. On the contrary, when the token is in $p_{on,2}$, only $t_{c,2}$ is enabled.

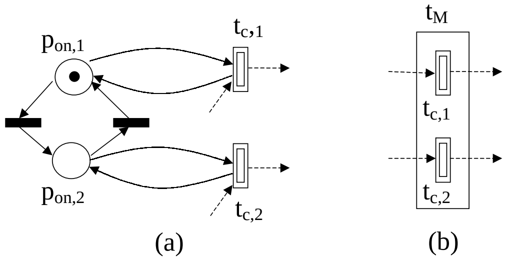

Figure 3: *The Petri net model of a macro transition: (a) detailed representation, (b) simplified representation.*

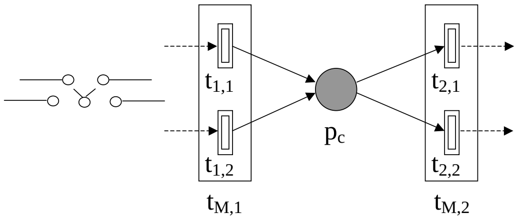

Figure 4: *A MIMO switch with* 2 *input and* 2 *output lines.*

Transportation lines and switches: Transportation lines consist of pipes of appropriate diameter, depending on the bottle sizes, where bottles are conveyed at a very high speed thanks to the force produced by the compressed air. Due to the high speed, the main feature of these elements is that there is no accumulation of bottles in their inside. Therefore, transportation lines may be seen as connecting elements and the corresponding places in the Petri net model are zero capacity places, i.e., places in P_0.

In the general scheme the connections among different lines may vary: this corresponds to a switch that can be of different types: MIMO (multi input - multi output), MISO (multi input - single output) and SIMO (single input - multi output). In the MIMO case, we represent a switch with a macro transition at the input and a macro transition at the output, thus enabling one possible path at a time. In Figure 4 a MIMO switch is represented in the case of two input and two output lines, where place p_c has been denoted as a dark circle because it is a zero capacity place.

Note that the position of the switch at the different time instants is a decision variable and should be established so as to optimize the performance of the whole plant.

Machines: In this plant we have two different types of machines. The first type produces bottles, while the second one fills and corks them.

Machines of the first type are equipped so as to produce bottles of different sizes. In the following, we consider the case of a machine that can be used to produce 1.5 ℓ bottles and 2 ℓ bottles. A detailed and a reduced scheme of the Petri net model for such a machine is shown in Figure 5. In particular, the firing of $t_{c,1}$ denotes the production of 1.5 ℓ bottles, whereas the firing of $t_{c,2}$ denotes the production of 2 ℓ bottles. Clearly, the productivity of the machine is not the same in the two cases, thus the maximum firing

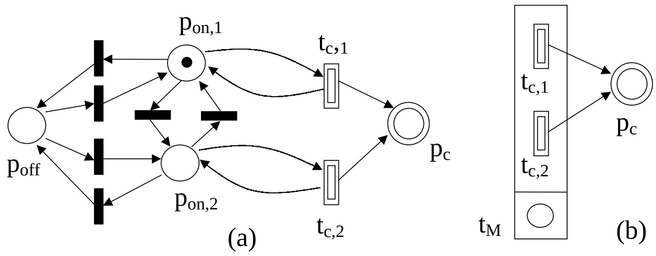

Figure 5: *The Petri net model of a machine that produces bottles: (a) detailed representation, (b) simplified representation.*

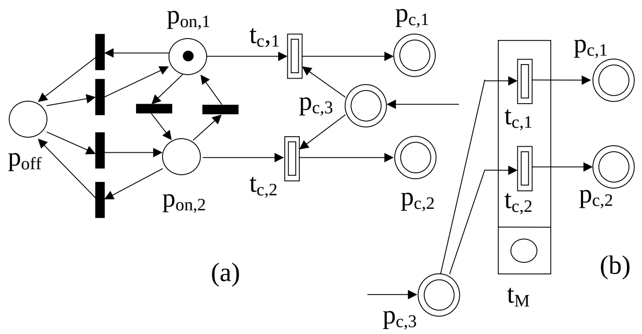

Figure 6: *The Petri net model of a machine that fills bottles: (a) detailed representation, (b) simplified representation.*

speed of transitions $t_{c,1}$ and $t_{c,2}$ are different, while the minimum firing speed is equal to zero in both cases. Note that this machine may also be turned off (when p_{off} is marked): thus three discrete places have been introduced in the detailed Petri net model. In the compact representation the presence of the place p_{off} is denoted by one empty circle at the bottom of the macro-transition.

Let us finally observe that as in the previous model, the firing delays associated to discrete transitions, as well as the initial configuration of the net, are design parameters. This means that controlling the plant implies to establish a priori when bottles of different formats should be produced. An additional degree of freedom is the speed at which each machine works when it is operational. This value is chosen so as to optimize a given performance index that usually coincide with the throughput of the net. In terms of Petri net model this is equivalent to select the instantaneous firing speed of continuous transitions $t_{c,1}$ and $t_{c,2}$ among the set of admissible IFS vectors.

A dual scheme may be used to describe the functioning of those machines that are used for bottles filling and corking. An example in the case of bottles of two different sizes is reported in Figure 6. A macro transition with an empty circle is used again to denote that the machine may also be off. Once again the firing delays associated to discrete transitions, the initial condition of the net, and the instantaneous firing speeds of continuous transitions are decision parameters.

Buffers: A Petri net model of a buffer is reported in Figure 7 in the case that bottles

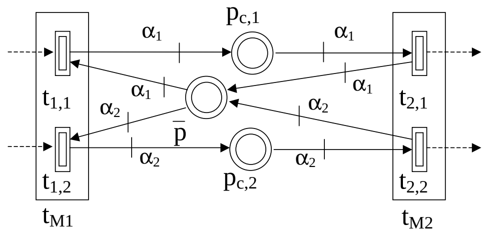

Figure 7: *The simplified Petri net model of a buffer.*

of two different sizes may be stored in it. For brevity's requirements the detailed model has been omitted, but it can be easily deduced, given the detailed model of a macro transition. When effectively modeling a buffer we should take into account all sizes of bottles that can be stored in it. This can be easily done by simply introducing a continuous place for each possible format (see places $p_{c,1}$ and $p_{c,2}$). Then, an additional place ($\overline{p}$) should also be introduced to limit the total volume of bottles entering the buffer, according to its capacity. In this place the fluid content is complementary to the whole content of the buffer, i.e., it is empty when the buffer is full and is full when the buffer is empty. Clearly, the total number of bottles that can be introduced in the buffer depend on their size, and this is taken into account through the different values of α_1 and α_2. Moreover, we should also impose that bottles of different sizes are not put together. This implies that the following conditions should be verified:

- if $m(p_{c,1}) > 0$, then $t_{1,2}$ is not enabled;
- if $m(p_{c,2}) > 0$, then $t_{1,1}$ is not enabled.

These are safeness specifications that may be structurally enforced in the net (e.g., by inhibitory arcs) or may be imposed on-line by a supervisory controller.

4 The FOHPN model of a real bottling plant

In this section we first describe a part of the whole production process of a real bottling plant in Sardinia we already considered in [5, 15]. Then, we show how it can be modeled through FOHPN by simply putting together the previous elementary modules.

Plant description: Let us consider the flow diagram sketched in Figure 8. It consists of seven machines ($M_1, \cdots, M_7$), 7 buffers ($B_1, \cdots, B_7$) and 13 switches ($s_1, \cdots, s_{13}$).

In this paper for sake of simplicity we focus our attention only on a part of the whole production plant. This is not a limitation: the rest of the plant can be similarly modelled using the modules described in the previous sections. In particular, we provide the hybrid Petri net model of the production line that starts from machine M_1, terminates with machines M_2, M_3, M_4, and uses buffers $B_1, \cdots, B_7$. Machines M_5, M_6 and M_7 have been neglected in the modeling phase. They have been reported here for sake of completeness,

	M_1	M_2	M_3	M_4	M_5	M_6	M_7
1.5 ℓ	6000	23000	20000	18000	10000	7800	3600
2 ℓ	5600	17000	15000	16000	9800	7600	$--$

Table 1: *Nominal productivity of the machines [bottles/hour].*

	B_1	B_2	B_3	B_4	B_5	B_6	B_7
1.5 ℓ	210000	31500	31500	31500	31500	31500	36750
2 ℓ	120000	18000	18000	18000	18000	18000	21000

Table 2: *Nominal capacity of the buffers [bottles].*

because they interact with the considered production line as shown in Figure 8. This is the reason why a dashed line has been used to represent them, as well as an arrow, instead of a continuous line, has been used to represent the connecting elements joining them to the rest of the production line.

The first stage of the considered production cycle consists in the creation of the PET bottles, while the last stage consists in filling and corking them. More precisely, the first operational machine is M_1 that produces PET bottles starting from raw-material of PET granules (PET chips). Thanks to an appropriate equipment, this machine may be extremely versatile and may produce different bottle sizes, e.g., 1.5 ℓ and 2 ℓ. In Figure 8 the flow of 1.5 ℓ bottles has been represented with a continuous green line, while the flow of 2 ℓ bottles has been represented with a dashed red line. The produced bottles are directed to appropriate lines of different diameter, depending on their size. The flow of bottles through the conveyor lines occurs at a high speed and is induced by a jet of compressed air. Bottles may follow different paths and may be assigned to different buffers. Path assignment may be seen as a decision problem whose solution aims to optimize the production process. In particular, in the production line we are dealing with, there are 7 buffers ($B_1, \cdots, B_7$) and the assignment is established so as to compensate as much as possible the delay due to the reduced productivity of the machines that fill bottles of mineral water with respect to those that produce them.

Finally, from the buffers bottles are conveyed to the zone of self–filling through other appropriate flow lines. Even in this case, bottles may follow different paths so as to better exploit the filling machines. In particular, there are 3 filling machines that are denoted in Figure 8 as M_2, M_3 and M_4, and that can be used to fill bottles of all sizes.

The nominal productivity of the different machines, in terms of number of bottles that can be produced (filled) in one hour, are reported in Table 1. Finally, in Table 2 we have reported the capacity of the buffers. Clearly, both the productivity of the machines and the capacity of the buffers, depend on the considered format.

The FOHPN model: The FOHPN model of the above production process has been reported in Figure 9, where all the elementary modules previously defined can be easily recognized. The same colour notation has been used in the two figures, so as to better distinguish the flow of bottles of different sizes, and their flow in the belt conveyor. We may also observe that all continuous places with a zero capacity have been denoted as full dark circles.

Note that two further colours with respect to those in Figure 8, namely blue and yellow, have been introduced in Figure 9 to denote that machine M_4 is also used for filling and corking bottles of two other sizes, namely 0.5 and 1 ℓ.

5 Simulation results

In this section we show how the FOHPN model of the production line can be efficiently used to carry out some numerical simulation. In particular, we consider a certain number of operating configurations, that are the most commonly used by the plant operators, and we show how, among these configurations, it is possible to identify the best one in terms of a given performance index.

All simulations have been carried out using Simulink, a Toolbox of Matlab particularly suited when dealing with large scale and modular systems, like the one of interest here. Details on the simulation model are omitted here for sake of brevity but can be found in [4].

The Petri net model of the considered production line is reported in Figure 9 and represents only a part of the whole production process. Note however that the presence of the dashed arcs coming from other production lines enables us to take into account the effect of the rest of the production plant, namely machines M_5, M_6, and M_7 as shown in Figure 8.

As already mentioned in the previous section the design parameters that characterize an operating condition of the plant are the following:

- the initial configuration of the plant, i.e., the initial marking of the net;
- the paths that bottles should follow at the different time intervals, i.e., the firing delays associated to discrete transitions in the Petri net model of switches;
- the time intervals at which machines should produce (fill) bottles of different formats, i.e., the firing delays associated to discrete transitions in the Petri net model of machines producing (filling) bottles.
- the productivity rate of machines producing and filling bottles, namely the instantaneous firing speed of continuous transitions modeling the machine operation.

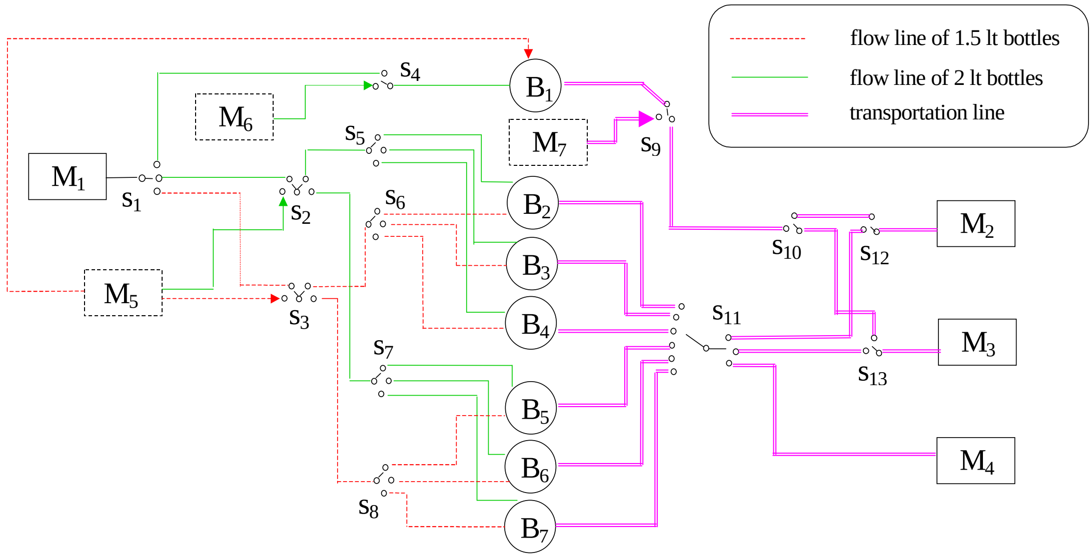

Figure 8: *A scheme representing a part of the bottling production process.*

In the considered application we assume that the instantaneous firing speeds of continuous transitions are selected among the set of admissible IFS so as to optimize the throughput of the net. This implies that in the case of machines producing bottles we may always assume that when these machines are operational, they always work at their nominal productivity. In terms of Petri net model this means that when a continuous transition modeling the machine operation (namely, $t_{c,1}$ or $t_{c,2}$ in Figure 5) fires, it always fires at its maximum firing speed, regardless of the actual marking of the net. This is no longer valid in the case of machines filling bottles because of their higher productivity. Therefore, in the case of machines M_2, M_3 and M_4 we first establish in which time intervals they can fill bottles of a given format: within these time intervals machines work at a firing speed, that may not coincide with their maximal firing speed (MFS), i.e., with the productivity of the machine, but may be smaller and strictly related both to the velocity at which bottles are produced by the upstream machines and to the actual configuration of the net. In particular, filling machines cannot work at their nominal productivity when the upstream buffers are empty. On the contrary, if buffers are full filling machines may work at their nominal productivity, or equivalently continuous transitions may fire at their MFS. In other words, when the upstream buffers are empty continuous transitions modelling filling machines are weakly enabled, while they are strongly enabled when buffers are full.

Different numerical simulations have been carried out using the real data of the machines (namely, their productivity) and the buffers (namely, their maximum capacity). In the following we focus our attention on 1.5 and 2 ℓ bottles. In particular, we consider 8 different working conditions that are typical according to the plant operators.

Note that in all cases examined we assumed that all buffers are initially empty.

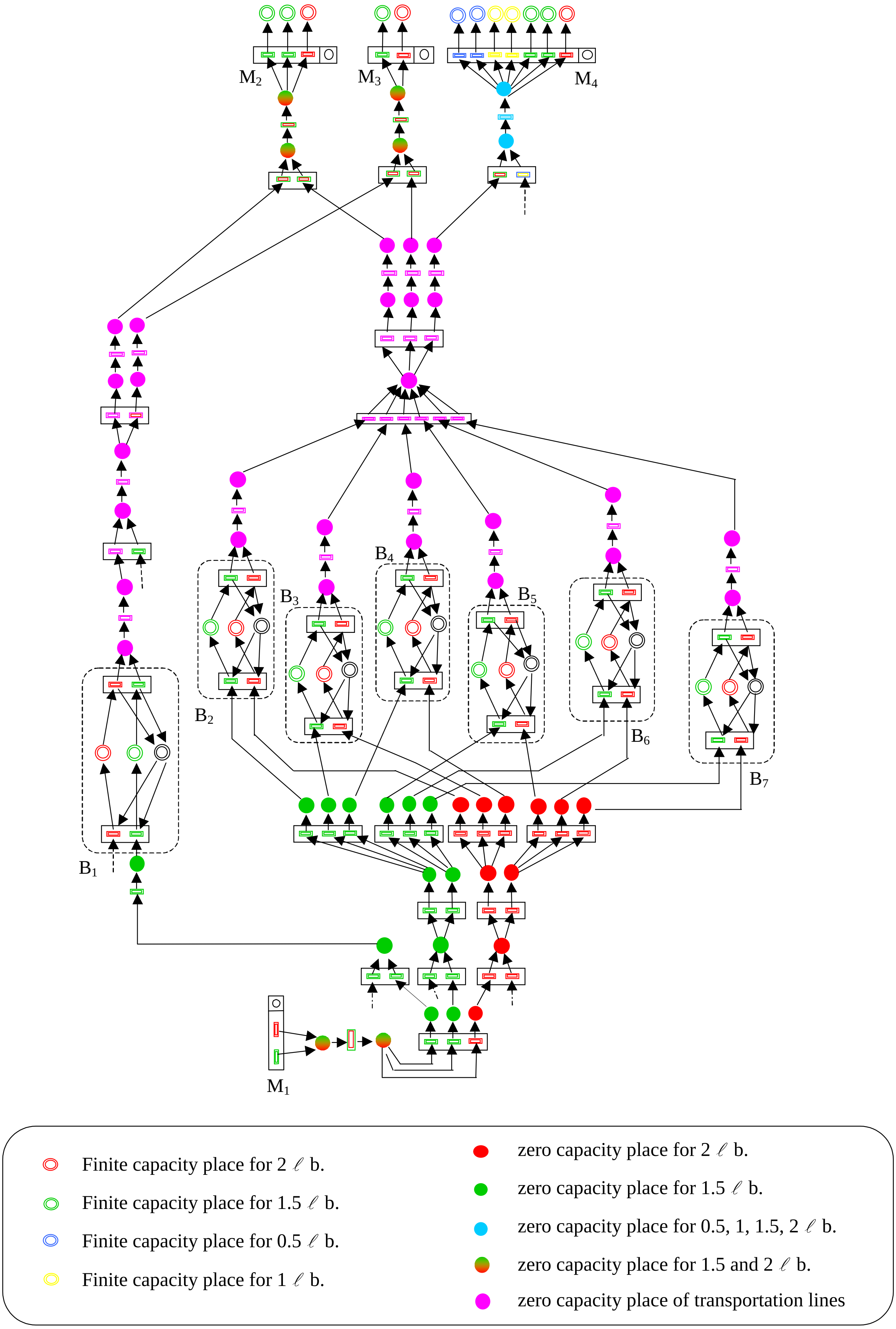

Figure 9: *The Petri net model of the production process in Figure 8.*

	Case 1	**Case 2**	**Case 3**	**Case 4**
Production Machines	M_1 [1.5 ℓ(50%), 2 ℓ(50%)]	M_1 [1.5 ℓ(50%), 2 ℓ(50%)] M_6 [1.5 ℓ(100%)]	M_1 [1.5 ℓ(100%)] M_5 [1.5 ℓ(100%)]	M_1 [1.5 ℓ(90%), 2 ℓ(10%)] M_5 [1.5 ℓ(100%)] M_6 [1.5 ℓ(50%), 2 ℓ(50%)] M_7 [1.5 ℓ(100%)]
Buffers	B_1, B_2, B_3	B_1, B_2, B_3	B_1, B_2	B_1, B_2, B_3, B_4, B_5, B_6, B_7
Filling machines	M_2 [1.5 ℓ(40%), 2 ℓ(60%)]	M_2 [1.5 ℓ(100%)] M_3 [1.5 ℓ(100%)] M_4 [2 ℓ(100%)]	M_2 [1.5 ℓ(100%)] M_3 [1.5 ℓ(100%)]	M_2 [1.5 ℓ(100%)] M_3 [1.5 ℓ(100%)] M_4 [2 ℓ(100%)]
Switches	s_1, s_2, s_4, s_5, s_9, s_{10}, s_{11}, s_{12}, s_{13}	s_1, s_2, s_3, s_4, s_5, s_6, s_9, s_{10}, s_{11}, s_{12}, s_{13}	s_1, s_2, s_3, s_4, s_5, s_6, s_9, s_{10}, s_{11}, s_{12}, s_{13}	s_1, s_2, s_3, s_4, s_5, s_6, s_7, s_8, s_9, s_{10}, s_{11}, s_{12}, s_{13}

	Case 5	**Case 6**	**Case 7**	**Case 8**
Production Machines	M_1 [1.5 ℓ(50%), 2 ℓ(50%)] M_5 [1.5 ℓ(77%), 2 ℓ(23%)] M_6 [1.5 ℓ(100%)]	M_1 [1.5 ℓ(50%), 2 ℓ(50%)] M_5 [2 ℓ(100%)] M_7 [1.5 ℓ(100%)]	M_1 [1.5 ℓ(20%), 2 ℓ(80%)] M_5 [1.5 ℓ(100%)]	M_1 [1.5 ℓ(50%), 2 ℓ(50%)] M_5 [2 ℓ(100%)]
Buffers	B_1, B_2, B_7	B_1, B_2, B_3	B_1, B_2, B_3, B_4, B_5, B_6, B_7	B_1, B_2
Filling machines	M_2 [1.5 ℓ(100%)] M_3 [1.5 ℓ(100%)] M_4 [2 ℓ(100%)]	M_2 [1.5 ℓ(100%)] M_3 [2 ℓ(100%)] M_4 [2 ℓ(100%)]	M_2 [1.5 ℓ(100%)] M_3 [1.5 ℓ(100%)] M_4 [2 ℓ(100%)]	M_2 [2 ℓ(100%)] M_3 [1.5 ℓ(100%)]
Switches	s_1, s_2, s_3, s_4, s_5, s_7, s_8, s_9, s_{10}, s_{11}, s_{12}, s_{13}	s_1, s_2, s_3, s_4, s_5, s_6, s_9, s_{10}, s_{11}, s_{12}, s_{13}	s_1, s_2, s_3, s_4, s_5, s_6, s_7, s_8, s_9, s_{10}, s_{11}, s_{12}, s_{13}	s_1, s_2, s_3, s_4, s_5, s_6, s_9, s_{10}, s_{11}, s_{12}, s_{13}

Table 3: *The main features of the considered numerical simulations.*

In Table 3 we have summarized the main features of the considered numerical simulations: we have specified which are the machines involved in the production of bottles and the percentage of the production time dedicated to each format; the buffers where bottles are stored; the machines used for filling bottles and the percentage of the production time dedicated to each format; the switches where the flow of bottles really occurs. More details about the considered numerical simulations, have only been reported for Case 5 that, as shown in the following, corresponds to the optimal working configuration among the considered ones, according to some performance criteria. Details about the other cases have not been reported here for sake of brevity, but can be read in [4].

Note that in all cases we considered a time period of simulation that is equal to 48 hours. This choice originates from the observation that, in *all* the considered cases, 48 hours is the interval of time over which the evolution repeats identically.

Example 4 Let us now consider Case 5 of Table 3. The decision parameters for Case 5 are reported in Table 4. More precisely, in this table we have reported:

- the time intervals where each machine producing bottles is involved in the production of a given format;
- the time intervals where machines filling bottles may operate on a given format;
- the time intervals where the flow of bottles trough a given switch may occur.

As an example, from this table we can argue that machine M_1 is operational for 42 hours over the whole period of simulation. In particular, the first 11 hours are devoted to the production of 1.5 ℓ bottles, then the machine stops working for an hour, then it produces 2 ℓ bottles for the successive 11 hours, and so on. We can also argue that the position of switch s_1 is such that during the first 12 hours of simulation the flow of bottles may occur from machine M_2 towards switch s_2, then in the successive 12 hours, bottles may flow from machine M_1 towards switch s_3, and so on. Finally, each machine filling bottles may only operate on a given format, namely machines M_2 and M_3 may only fill 1.5 ℓ bottles, while machine M_4 may only fill 2 ℓ bottles. ■

The results of the considered simulations, in terms of throughput and net profit, are summarized in Figures 10 and 11.

Figure 10 shows the number of 1.5 ℓ and 2 ℓ bottles ($N_{1.5}$ and N_2, respectively) produced in a time interval of 48 hours.

Clearly, the main goal of the company is that of maximizing the net profit resulting from selling its end items. We first assume that all the produced bottles are sold. In such a case the net profit is

$$P = (SP_{1.5} - UC_{1.5}) \cdot N_{1.5} + (SP_2 - UC_2) \cdot N_2$$

where $SP_{1.5}$ (SP_2) is the *selling price* of 1.5 (2) ℓ bottles, while $UC_{1.5}$ (UC_2) is the *unitary cost* associated to 1.5 (2) ℓ bottles. The selling price is the price at which the end item is sold to a customer. In all numerical simulations we assumed $SP_{1.5} = 18\ c$ and $SP_2 = 22\ c$, where c denotes a cent of Euro. The unitary cost is the cost that the company pays for one unit of end item. It includes the cost that the company pays for the PET and the water, plus an additional term taking into account the production costs pertaining to one bottle. In particular, we assumed $UC_{1.5} = 5\ c$ and $UC_2 = 6\ c$.

The resulting net profit, computed under the assumption that all the produced bottles are sold, is that shown by the light (magenta) bars in Figure 11. Thus we can conclude that Case 5 corresponds to the best configuration of the plant with respect to the considered performance index P. By looking at Figure 10 we may also observe that Case 5 does not correspond to the maximal productivity of any format. This means that the maximum

	1.5 ℓ	2 ℓ
M_1	[0, 11], [24, 35]	[12, 23], [36, 47]
M_5	[0, 17], [24, 41]	[18, 23], [42, 47]
M_6	[17, 22], [41, 46]	

	Switches' position	Time intervals
s_1	$M_1 \to s_2$ $M_1 \to s_3$	[0, 12), [24, 36) [12, 24), [36, 48]
s_2	$s_1 \to s_5$ $M_5 \to s_7$	[0, 18), [24, 42) [18, 24), [42, 48]
s_3	$s_1 \to s_8$	[0, 48]
s_4	$M_6 \to B_1$	[0, 48]
s_5	$s_2 \to B_2$	[0, 48]
s_7	$s_2 \to B_7$	[0, 48]
s_8	$s_3 \to B_7$	[0, 48]
s_9	$B_1 \to s_{10}$ $M_7 \to s_{10}$	[0, 18), [24, 42) [18, 24), [42, 48]
s_{10}	$B_1 \to s_{10}$ $s_9 \to s_{12}$	[0, 18), [24, 42) [18, 24), [42, 48]
s_{11}	$B_2 \to s_{13}$ $B_7 \to M_4$	[0, 12), [24, 36) [12, 24), [36, 48]
s_{12}	$B_1 \to s_{10}$ $S_{10} \to M_2$	[0, 12), [24, 36) [12, 24), [36, 48]
s_{13}	$s_{11} \to M_3$	[0, 48]

	1.5 ℓ	2 ℓ
M_2	[0, 48]	
M_3	[0, 48]	
M_4		[0, 48]

Table 4: *The decision parameters for Case 5 as described in Example 4.*

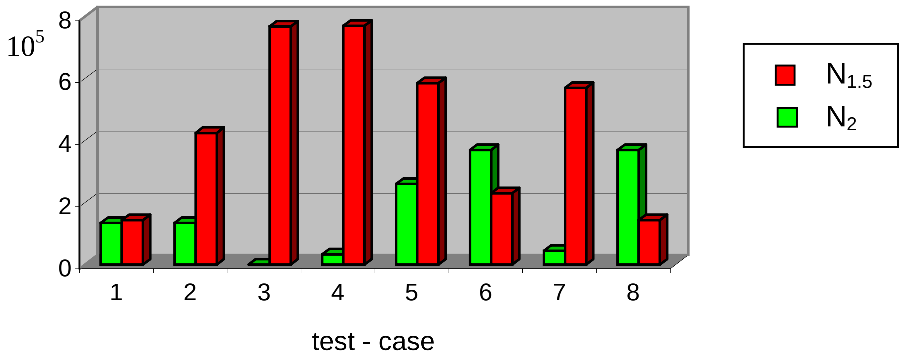

Figure 10: *The number of 1.5 ℓ ($N_{1.5}$) and 2 ℓ (N_2) bottles produced at the considered operating conditions.*

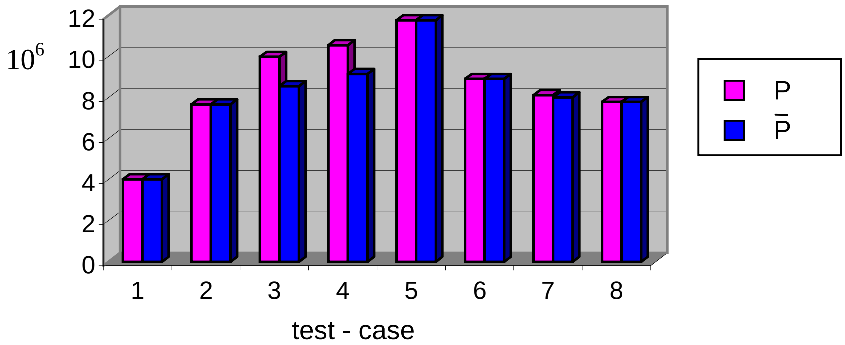

Figure 11: *The net profit P under the assumption that all bottles are sold and the net profit $\overline{P}$ taking into account some constraints in the sale.*

profit is guaranteed by appropriately partitioning the production resources among bottles of different sizes.

Finally, we compute the net profit under the following two realistic assumptions. Firstly, we assume that there is an upper bound on the demand of bottles of each format: if the number of produced bottles is greater than such a limit, then there is a certain number of bottles that are not sold, thus producing no profit. Secondly, we assume that if the number of bottles is less than a given lower bound then the whole demand cannot be met. This produces a *shortage* which usually has many associated costs. Apart from the loss of profit, the effects of shortage include loss of goodwill, loss of future sales, and so on. In particular, in all numerical simulations we assumed that within the considered time period of simulation, the maximum number of bottles of each format that can be sold is $N_{\max} = 7 \cdot 10^5$, while the number of produced bottles under which there is shortage is $N_{\min} = 10^5$. Finally, we evaluated that shortage cost is equal to $SC = 2\ c$ for unit of end item for both formats. In such a case the net profit is equal to

$$\begin{aligned}\overline{P} &= SP_{1.5}\cdot\min\{N_{1.5},N_{\max}\}-UC_{1.5}\cdot N_{1.5}-SC\cdot\max\{0,N_{\min}-N_{1.5}\}\\ &\quad +SP_2\cdot\min\{N_2,N_{\max}\}-UC_2\cdot N_2-SC\cdot\max\{0,N_{\min}-N_2\}.\end{aligned}$$

When the performance index to be maximized is $\overline{P}$, the resulting histogram is given by the dark (blue) bars in Figure 11. Thus we can conclude that even in this case the best configuration of the plant is the fifth one.

Example 5 Let us consider again Case 5 whose decision parameters have been reported in Table 4. In Table 5 we have summarized the simulation results for this case, namely the time intervals at which the flow of bottles "really" occurs in the transportation lines, depending on the switches' position, and the productivity of filling machines at the different time intervals of operation. ■

6 Conclusions

In this paper we have shown how FOHPN can be efficiently used to model the dynamic behavior of a mineral water bottling plant. One important feature of the proposed model consists in allowing the fluid approximation of some discrete event dynamics. Thanks to this, we have been able to provide some numerical simulations. In particular, we focused our attention on the most commonly used working configurations and we show how thanks to simulation, we can identify among them the best configuration in terms of net profit, also taking into account shortages costs.

Our future efforts in this area will be devoted to a careful analysis of optimization via simulation and to perform sensitivity analysis using the analytical properties of the FOHPN model.

References

[1] M. Ajmone Marsan, G. Balbo, G. Conte, S. Donatelli, G. Franceschinis, *Modelling with Generalized Stochastic Petri Nets*, Wiley Series in Parallel Computing, John Wiley and sons, 1995.

[2] H. Alla, R. David, "Continuous and hybrid Petri nets," *Journal of Circuits, Systems, and Computers*, vol. 8, no. 1, February 1998. p. 159-88.

[3] H. Alla, R. David, "A modeling and analysis tool for discrete events systems: continuous Petri net," *Performance Evaluation*, Vol. 33, no. 3, 1998, p. 175-99.

[4] R. Armosini, "Simulation of the production process of a bottling plant using hybrid Petri nets and Simulink," *Laurea Thesis*, Dep. of Electrical and Electronic Engineering, University of Cagliari, Italy, 2002, (in Italian).

	Switches' position	Flow of bottles [hours]	Format
s_1	$M_1 \rightarrow s_2$ $M_1 \rightarrow s_3$	[0, 11], [24, 35] [12, 23], [36, 47]	1.5 ℓ 2 ℓ
s_2	$s_1 \rightarrow s_5$ $M_5 \rightarrow s_7$	[0, 11], [24, 35] [18, 23], [42, 47]	1.5 ℓ 2 ℓ
s_3	$s_1 \rightarrow s_8$	[12, 23], [36, 47]	2 ℓ
s_4	$M_6 \rightarrow B_1$	[0, 5], [24, 29]	1.5 ℓ
s_5	$s_2 \rightarrow B_2$	[0, 11], [24, 35]	1.5 ℓ
s_7	$s_2 \rightarrow B_7$	[18, 23], [42, 47]	2 ℓ
s_8	$s_3 \rightarrow B_7$	[12, 23], [36, 47]	2 ℓ
s_9	$B_1 \rightarrow s_{10}$	[0, 17], [24, 41]	1.5 ℓ
s_{10}	$B_1 \rightarrow s_{10}$	[0, 17], [24, 41]	1.5 ℓ
s_{11}	$B_2 \rightarrow s_{13}$ $B_7 \rightarrow M_4$	[0, 11], [24, 35] [12, 23], [36, 47]	1.5 ℓ 2 ℓ
s_{12}	$B_1 \rightarrow s_{10}$	[0, 17], [24, 41]	1.5 ℓ
s_{13}	$s_{11} \rightarrow M_3$	[0, 11], [24, 35]	1.5 ℓ

	1.5 ℓ bottles' filling [hours]	2 ℓ bottles' filling [hours]	Productivity [bottles/hour]
M_2	[0, 5), [24, 29)		17800
	[5, 17], [29, 41]		10000
M_3	[0, 11], [24, 35]		6000
M_4		[12, 18], [36, 42]	5600
		[18, 23], [42, 47]	15400

Table 5: *Details simulation results for Case 5 as described in Example 5.*

[5] R. Armosini, A. Giua, M.T. Pilloni, C. Seatzu, "Simulation and control of a bottling plant using First-Order hybrid Petri nets," *Proc. First Multidisciplinary International Symposium on Positive Systems: Theory and Applications*, pp. 79-86, Rome (Italy), August 2003.

[6] F. Baccelli, G. Cohen, G. Olsder, J. Quadrat, *Synchronization and linearity*, Wiley, 1992

[7] F. Balduzzi, A. Giua, G. Menga, "First–Order Hybrid Petri Nets: a model for optimization and control," *IEEE Trans. on Robotics and Automation*, Vol. 16, No. 4, pp. 382-399, August, 2000.

[8] F. Balduzzi, A. Giua, C. Seatzu, "Modelling and simulation of manufacturing systems using First-Order Hybrid Petri Nets," *Int. Journal of Production Research*, Vol. 39, No. 2, pp. 255-282, January 2001.

[9] L. Benvenuti, L. Farina, "Positive and compartmental systems," *IEEE Trans. on Automatic Control*, Vol. 47, No. 2, pp. 370-373, February, 2002.

[10] G. Cohen, S. Gaubert, J. Quadrat, "Max-plus algebra and system theory : where we are and where to go now," *Annual Reviews in Control*, Vol. 23, pp. 207–219, 1999.

[11] J.M. Colom, M. Silva, "Improving the linearly based characterization of P/T nets," *Advances in Petri Nets 1990*, Lecture Notes in Computer Sciences, vol. 483, pp. 113–145, Springer-Verlag, 1991.

[12] I. Demongodin, "Generalised batches Petri net: hybrid model for high speed systems with variable delays," *Discrete Event Dynamic Systems: Theory and Applications*, vol. 11, no. 1/2, pp. 137-162, January/April 2001.

[13] A. Di Febbraro, A. Giua, G. Menga, (eds.) "Special issue on hybrid Petri net," *Discrete Event Dynamic Systems: Theory and Applications*, vol. 11, no. 1/2, January/April 2001.

[14] R. Furcas, Giua A., Piccaluga A., Seatzu C., "Hybrid Petri net modeling of inventory management systems," *European Journal of Automation APII-JESA*, vol. 35, no. 4, 2001, p. 417-434.

[15] A. Giua, A. Meloni, M.T. Pilloni, C. Seatzu, "Modeling of a bottling plant using hybrid Petri nets," *2002 IEEE Int. Conf. on Systems, Man and Cybernetics*, Hammamet (Tunisia), October 2002.

[16] T. Murata, "Petri nets: properties, analysis and applications," *Proceedings IEEE*, Vol. 77, No. 4, pp. 541–580, 1989.

[17] Y.A. Phillis, V.S. Kouikoglou, "Discrete event modeling and optimization of unreliable production lines with random rates," *IEEE Trans. Robotics and Automation*, Vol. 10, No. 1, pp. 153–159, 1994.

[18] A. Sharifnia, "Stability and performance of distributed production control methods based on continuous–flow models," *IEEE Trans. Automatic Control*, Vol. 39, No. 4, pp. 725–737, 1994.

[19] M. Silva, L. Recalde, "Petri nets and integrality relaxations: a view of continuous Petri nets," *IEEE Trans. on Systems, Man, and Cybernetics*, Vol. 32, No. 4, 2002.

[20] R. Suri, B.R. Fu, "On using continuous flow lines to model discrete production lines," *J. Discrete Event Dynamic Systems*, No. 4, pp. 129–169, 1994.